Phosphorus Recovery from Microbial Biofuel Residual Using Microwave Peroxide Digestion and Anion Exchange

McKay Gifford[a*], Jianyong Liu[b], Bruce E. Rittmann[c], Raveender Vannela[c], Paul Westerhoff[a]

[*]Corresponding author:

[a]Arizona State University, School of Sustainable Engineering and The Built Environment, Tempe, Box 5306, AZ 85287-5306; phone: 480-965-2885; fax: 480-965-0557; email: mac.gifford@asu.edu

Affiliations

[a]Arizona State University, School of Sustainable Engineering and the Built Environment, Tempe, AZ 85287-5306

[b]School of Environmental and Chemical Engineering, Shanghai University, 333 Nanchen Road, Shanghai 200444, P. R. China

[c]Arizona State University, Swette Center for Environmental Biotechnology, Biodesign Institute, Tempe, AZ 85287-5701

Last revision: November 10, 2014

In preparation for: *Water Research* (Elsevier)

Abstract

Sustainable production of microalgae for biofuel requires efficient phosphorus (P) utilization, which is a limited resource and vital for global food security. This research tracks the fate of P through biofuel production and investigates P recovery from the biomass using the cyanobacterium *Synechocystis* sp. PCC 6803. Our results show that *Synechocystis* contained 1.4% P dry weight. After crude lipids were extracted (e.g., for biofuel processing), 92% of the intracellular P remained in the residual biomass, indicating phospholipids comprised only a small percentage of cellular P. We estimate a majority of the P is primarily associated with nucleic acids. Advanced oxidation using hydrogen peroxide and microwave heating released 92% of the cellular P into orthophosphate. We then recovered the orthophosphate from the digestion matrix using two different types of anion exchange resins. One resin impregnated with iron nanoparticles adsorbed 98% of the influent P through 20 bed volumes, but only released 23% during regeneration. A strong-base anion exchange resin adsorbed 87% of the influent P through 20 bed volumes and released 50% of it upon regeneration. This recovered P subsequently supported growth of *Synechocystis*. This proof-of-concept recovery process reduced P demand of biofuel microalgae by 54%.

Keywords

Microbial Biofuel, Phosphorus Recovery, Oxidation, Anion Exchange, Iron Nanoparticles

1. Introduction

There is an urgent need to find energy replacements for fossil fuels, whose combustion releases known and suspected human carcinogens and greenhouse gases into the atmosphere. One promising alternative is biofuel, which provides renewable energy with net greenhouse gas emissions significantly lower than fossil fuel (Batan et al. 2010). Biofuel derived from microalgae offers several advantages over biofuel from terrestrial plants: it does not compete with food crops for arable land, it can be continuously harvested, and it provides a much higher areal yield (Rittmann 2008, Schenk et al. 2008).

Microalgae biofuel production requires several inputs, including water, sunlight, carbon dioxide, and nutrients – particularly nitrogen (N) and phosphorus (P). During lipid extraction from microalgae biomass for liquid fuels, most of the N and P are discarded, requiring new nutrients for subsequent growth. Should microalgae become a significant replacement for fossil fuel in the future, the requirements for biomass growth would create a huge nutrient demand, rivaling that of agriculture (Erisman et al. 2010). Thus, capturing and recycling nutrients represents a significant opportunity for making large-scale cultivation of microalgae more sustainable (Clarens et al. 2010).

Nutrient recycling is particularly essential for P. Unlike N, which can be fixed from the atmosphere through the Haber-Bosch method (Huo et al. 2012), P is mined from ore that has finite stocks. World reserves of accessible P are estimated as 65,000 million

---

Abbreviations: ATP, adenosine triphosphate, DI, deionized water; EBCT, empty bed contact time; FAME, fatty acid methyl esters; HAX, hybrid anion exchange; ortho-PO_4^{3-}, orthophosphate; P, phosphorus; PG, phosphatidylglycerol; SBAX, strong base anion exchange.

63 metric tons (USGS 2011), and these are non-renewable and not substitutable. Depletion
64 of economically affordable P may bring about international crises due to the essential role
65 of P fertilizer for global food production (Cordell et al. 2009). Farmers in developing
66 countries could be disproportionately harmed (Childers et al. 2011). Sustainable microbial
67 biofuel production demands efficient nutrient recycling to prevent biofuel from becoming
68 an enormous P demand competing with food production.
69 This research develops a proof-of-concept process for P-recovery from microalgae
70 after extraction of lipids. The research objective is to track P through biofuel production
71 and then recover P from residual biomass in a reusable form by using advanced oxidation
72 to release the P for efficient ion exchange capture. The reusable form provides
73 bioavailable P that supports microalgae growth.
74 We selected the cyanobacteria for this work because it is an excellent candidate for
75 future utilization in large-scale biomass cultivation, particularly when energy efficiency in
76 biosynthesis of fatty acids is crucial (Wijffels et al. 2013). Specifically we use
77 *Synechocystis* sp. PCC 6803, which is a prokaryotic autotroph, Gram negative and able to
78 withstand a wide range of environmental conditions. Lipids in the form of diacylglycerols
79 are available in an extensive network of thylakoid membranes (van de Meene et al. 2006,
80 Vermaas 2001). It may be genetically manipulated for specific traits favorable for biofuel
81 production such as high lipid content (Vermaas 1996) because the entire genome has been
82 sequenced (Kaneko et al. 1996).
83
84 *1.1. P Recovery*

To recover P from microbial biomass we first release organic-bound P as inorganic orthophosphate (ortho-PO_4^{3-}). This is necessary to improve the efficiency of the subsequent capture since ortho-PO_4^{3-} is more reactive. It also mitigates heterotrophic contamination of the biomass culture, which can occur after long run periods or with accumulation of inactive cells (Mata et al. 2010). Subsequently, we selectively capture the ortho-PO_4^{3-} from the liquid in a usable form. This is necessary to isolate and purify the ortho-PO_4^{3-}, allowing accurate and controlled dosing into the aqueous growth media during reuse. It also concentrates the ortho-PO_4^{3-} solution to minimize handling or hauling. This subsection gives the impetus for the technologies we selected to accomplish those goals.

Many P-recovery methods are available (de-Bashan and Bashan 2004, Morse et al. 1998, Rittmann et al. 2011). We selected an advanced oxidation process using hydrogen peroxide and microwave heating to release organic P from the residual biomass. Advanced oxidation creates hydroxyl free radicals that are highly effective for attacking organic matter to release ortho-PO_4^{3-} (Liao et al. 2005). This transformation may involve oxidation and hydrolysis reactions. While it may be possible to find technologies that are less energy-intensive, such as enzymatic hydrolysis or microbial fuel cells (Rittmann et al. 2011), or that do not dilute the biomass with additional liquid such as supercritical carbon dioxide (Blocher et al. 2012, Soh and Zimmerman 2011), advanced oxidation demonstrates the principle for releasing PO_4^{3-}.

We capture ortho-PO_4^{3-} using ion exchange since it recovers a liquid concentrate that is preferable for nutrient reuse during aquatic microalgae production. Other common recovery techniques such as aluminum adsorption or struvite precipitation (de-Bashan and Bashan 2004) produce complex or low solubility solids which may be better suited for

agricultural application. We evaluated two anion-exchange resins having distinctly different properties. The first was a hybrid anion exchange resin (HAX) impregnated with iron (hydr)oxide nanoparticles (Layne RT, Layne Christensen). It is reported to have a high sorption capacity and selectivity for ortho-PO_4^{3-} (Sengupta 2013) and the ability to release a high concentration ortho-PO_4^{3-} solution upon regeneration (Blaney et al. 2007, Midorikawa et al. 2008). The second was a type-1 strong-base anion exchange resin (SBAX) with quaternary amine functional groups in chloride ion form (21K-XLT, Dowex). It has a general anion-exchange capacity of 1.4 equivalents/L. It has previously been used for uranium (Stucker et al. 2011) and chromium (Rees-Nowak et al. 2005) removal, but has yet to be tested for phosphate recovery.

While the individual P recovery technologies employed in this study are not novel by themselves, their usage together such that the P completes an entire use and reuse cycle is. It is also the first study we know of to apply these technologies in the context of microbial biofuel production. Thus this study serves as a proof-of-concept that proposes an approach and can inform future optimization.

1.2. Microbial P

To focus the recovery efforts properly, this subsection estimates where P in *Synechocystis* is located based on literature review. Others have done this for several marine microalgae (Geider and La Roche 2002, Sterner and Elser 2002) but not specifically for *Synechocystis*. Biochemical fractions in cells can vary based on growth conditions (Sheng et al. 2011a) but this provides clues for understanding the fate of P after lipid processing. Figure 1 summarizes the expected location of P in a *Synechocystis* cell.

131 P may be located within adenosine triphosphate (ATP), lipids, and nucleic acid. The
132 following three paragraphs individually analyze them.

133 ATP contains over 18% P by weight ($C_{10}H_{16}N_5O_{13}P_3$), but comprises less than 30
134 µg per g of cell mass. P associated with ATP is therefore 5 µg per g of the cell mass,
135 which is a negligible contributor of the total cell P. The diphosphate form ADP and
136 monophosphate form AMP are smaller fractions of the cell mass with less incorporated P
137 and are also negligible contributors of cellular P storage.

138 The P content associated with lipid is a function of the fraction of lipid that is
139 phospholipid and the fraction of phospholipid that is P. The predominant phospholipid
140 head within cyanobacteria is phosphatidylglycerol (PG), which is the only phospholipid
141 associated with thylakoid membranes in *Synechocystis* sp. PCC 6803 (Hajime and Murata
142 2007). PG has an elemental composition of $C_8H_{12}O_{10}P$. The most prevalent fatty acid
143 chain in *Synechocystis* is C16:0, or palmitic acid (Sheng et al. 2011b), which has an
144 elemental composition of $C_{16}H_{32}O_2$. Assuming that all phospholipids within *Synechocystis*
145 are the diacylglycerol PG with two palmitic acid molecules, the overall elemental formula
146 for a phospholipid molecule is $C_{40}H_{76}O_{14}P$. That means phospholipid is approximately
147 3.8% P by weight. PG-based lipids comprise approximately 14% of all lipids in
148 *Synechocystis* (Sakurai et al. 2006), and lipids represent approximately 10% of the
149 biological makeup of the overall cell (Shastri and Morgan 2005). Combining these
150 estimates gives the theoretical amount of P associated with lipid in *Synechocystis* sp. PCC
151 6803 as 0.05% of the total cell weight, or 2% of the total cell P. A genetically altered high
152 lipid strain containing 50% crude lipids could then have as high as 0.3% of the total cell
153 weight be P associated with lipid. For this reason, we do not expect much P in the lipids.

We estimate the P content associated with DNA and RNA by comparing its biological composition with its elemental composition. *Synechocystis* sp. PCC 6803 is approximately 3% DNA and 17% RNA by weight (Shastri and Morgan 2005). DNA and RNA are 10% P by weight (Sterner and Elser 2002). Therefore, P associated with DNA comprises 0.3% of the total cell weight, and P associated with RNA is 1.7% of the total cell weight. This is respectively 15% and 83% of the total cellular P. We consequently expect that most of the cellular P will be in nucleic acid. This was also observed in other studies on lake bacteria where P associated with RNA comprised a majority of the total cell P (Elser et al. 2003, Geider and La Roche 2002).

2. Materials and Methods

2.1. Strain, Growth Conditions, and Biomass Production

We grew *Synechocystis* sp. PCC 6803 in BG-11 growth media (Rippka et al. 1979) modified to have five times the normal amount of phosphate (added as K_2HPO_4) (Kim et al. 2010) in a bench-top photobioreactor in semi-continuous growth mode. We separated biomass from the growth medium by means of centrifugation at 1,500 g for 20 min in 50-mL plastic tubes. We resuspended the cell pellet in 1 mM sodium bicarbonate (Sigma-Aldrich) to rinse away residual medium. We repeated centrifuging and rinsing two times before freeze-drying the final pellet (Labconco Freezone 6) for 2 days at 0.013 mbar and -50ºC in order to obtain an accurate starting dry weight (Sheng et al. 2011b). We collected enough biomass to perform all lipid extraction and P recovery experiments at least in duplicate.

177

178 *2.2. Lipid Extraction and Transesterification*

179 We extracted lipids from the freeze-dried biomass using the Folch Method (Folch
180 et al. 1957) using a 2:1 (V:V) mixture of chloroform (Mallinckrodt) and methanol (Fisher
181 Scientific), since it has a high extraction efficiency for *Synechocystis* lipids (Sheng et al.
182 2011b). We ground a 300-mg (all weights given as dry weight) sample with agate mortar
183 and pestle, suspended it in 60 mL of Folch solvent, and placed it on a shaker table at 175
184 rpm for 2 days. We filtered the suspension with a glass fiber filter (Whatman GF/B) and
185 then a 0.2-µm polytetrafluoroethylene filter (Whatman). The biomass retained on both
186 filters was the primary residual, and the filtrate contained the extracted crude lipid. For
187 samples undergoing transesterification, we evaporated the solvent from the crude lipid
188 under N_2 gas to avoid oxidation of lipids. For samples where no further lipid processing
189 was necessary, we evaporated the solvent by heating on hot plate.

190 We transesterified the crude lipid (Sheng et al. 2011b) by adding 1 mL of
191 methanolic hydrochloric acid (Supelco) and heating the mixture in an 85ºC water bath for
192 2 h. After cooling the mixture to room temperature, we added 0.5 mL of deionized (DI)
193 water and 1 mL of hexane, shook the mixture by hand for 30 s, and allowed the phases to
194 separate. We repeated all transesterification steps two additional times, and then pooled all
195 the hexane. The extracted hexane contained the fatty acid methyl esters (FAME), and the
196 remaining water contained the secondary residual.

197 For experiments tracking the fate of P, we analyzed total P for each biomass,
198 primary residual, crude lipid, secondary residual, and transesterified FAME (at least
199 duplicate samples).

200

201 *2.3. Advanced Oxidation*

202 We scraped primary residual from the dried filters and added it to 60 mL (giving
203 3.6 gVSS/L) of 30% ultrapure H_2O_2 solution (JT Baker Ultrex II) diluted 1:10. We let this
204 mixture stand for 1 hr of pre-digestion under fume-hood ventilation. We digested the
205 mixtures in a microwave (CEM MARS XPress) at 400 W by ramping the temperature up
206 to 170ºC over 10 min and then holding at 170ºC for 10 min per method SW846-3015
207 (USEPA 2008). Others have observed the highest fraction of P release by this peroxide
208 dose and microwave heating temperature (Liao et al. 2005, Wong et al. 2006), and future
209 work may explore varying other conditions to optimize P release. We employed high-
210 pressure microwave vessels to avoid breakage that the high rate of gas evolution could
211 cause. We analyzed duplicate samples before and after oxidation for total P and ortho-
212 PO_4^{3-}.

213

214 *2.4. Phosphate Separation*

215 We did preliminary investigation of the P separation capacity of each of the two
216 anion exchange resins by placing 3.5 g of fresh resin in a 1.5-cm inner diameter glass
217 column, giving a bed depth of 3.0 cm. We supported the resin with glass beads to ensure
218 even flow distribution. We flushed 100 mL of DI water through the column and allowed
219 air bubbles to escape. Then, we pumped a solution of monobasic sodium phosphate
220 (Mallinkrodt ACS grade) in DI water (concentration 80 mgP/L) through the column at 3.2
221 mL/min to give an empty bed contact time (EBCT) of approximately 2 min (loading rate of
222 4.4 mgP/s/g resin). We periodically took effluent samples for P analysis, and continued

223 the experiment until the effluent P concentration stabilized near the influent P
224 concentration. We then desorbed the P using a strong regeneration solution at a pump rate
225 of 0.5 mL/min (EBCT of approximately 10 min) until the effluent P concentration
226 stabilized at nearly zero. The strong regeneration solution used for the HAX resin was 0.1
227 N potassium hydroxide (EMD), and for the SBAX resin was 0.1 N sodium chloride (Sigma
228 Aldrich). We later varied influent P concentration, EBCT, P loading rate, influent pH, and
229 elute contact time in order to optimize column operation.

230 We then tested each resin with biomass after advanced oxidation by pumping the
231 60 mL of digested sample through 2.0 g of fresh resin having a bed depth of 1.7 cm. The
232 flow rate was 1.4 mL/min, giving an EBCT of approximately 2 min. We collected the
233 effluent and pumped it through the column two more times to ensure complete capture of
234 phosphate onto the resin. We then recovered retained ortho-PO_4^{3-} by removing the resin
235 from the column and placing it in 33 mL (11 bed volumes) of strong regeneration solution,
236 which was heated on a 95ºC hot plate, shaken for 24 h, and then decanted. Elution and
237 decanting were repeated two times, and the elution solutions were pooled so that the serial
238 batch elution mimicked a continually stirred tank mixer (CSTM) in series (n = 3). We
239 analyzed the total volume of 100 mL (33 bed volumes) for pH, total P, and ortho-PO_4^{3-}.

240 We obtained the total mass of P sorbed to each resin by summing the difference
241 between the influent concentration and the effluent concentration for each sample
242 multiplied by the volume treated in the time segment (area above the curve times flow
243 rate).

244

245 *2.5. Phosphorus Reuse*

As a confirmatory experiment, recovered P solution was used to culture wild-type *Synechocystis* sp. PCC 6803 cells. We diluted the recovered P solution to P concentration prescribed by standard BG-11, spiked the other nutrients to standard levels, then added additional bicarbonate to compensate for low aeration in small samples. We inoculated plastic tubes containing 20 mL of the growth media with fresh *Synechocystis* cells in duplicate. We placed these on a shake table under constant light conditions for one week, and regularly monitored optical density by absorbance at 730 nm.

2.6. Phosphorus Analysis

We determined ortho-PO_4^{3-} colorimetrically with a spectrophotometer (HACH DR5000) using the PhosVer 3 Method (HACH), which is equivalent to *Standard Methods* 4500-P.E (Miner 2006). It directs to add reagent powder to 5 mL of sample and give 2 min of reaction time, then measure results at 880 nm.

We assayed total P by persulfate digestion (*Standard Method* 4500-P.B.5) (Miner 2006) followed by inductively coupled plasma optical emission spectrometry (ICP-OES). To do this we suspended samples in 50 mL DI water plus 1 mL of concentrated sulfuric acid (JT Baker ultrapure). We then added 0.4 mg of ammonium persulfate (Malinckrodt) to each sample. We autoclaved the sample for 30 min at a pressure of 1.05 kg/cm^2 and a temperature of 122ºC. We measured total P by ICP-OES (Thermo iCAP6300) at a wavelength of 213.6 nm.

3. Results & Discussion

3.1. Fate of P through lipid extraction

269 Freeze dried *Synechocystis* sp. PCC 6803 biomass contained 1.39%±0.28% total P
270 by dry mass. (All weights given by dry weight. ± indicates half standard deviation.) This
271 is consistent with previous findings that P is 1.5% of dry cell mass (Kim et al. 2010). In
272 lipid-extracted biomass samples, primary residual contained 1.50%±0.36% total P by dry
273 mass. Figure 2 summarizes the fate of P through lipid extraction normalized to 100 mg of
274 total P in the starting biomass. The primary residual contained 92±4.3 mg total P. Crude
275 lipid contained 7.3±4.2 mg total P. For transesterified samples, total P in the FAME was
276 0.5±0.1 mg total P. Total P in the secondary residual was 9.5±5.3 mg. Thus, nearly all of
277 the starting organic P was in the primary residual after lipid extraction. Of the small
278 amount in the crude lipids, nearly all of it was in the secondary residual. Essentially no P
279 (<1% of the starting P) was in the transesterified FAME.
280 These findings support our expectation that nucleic acid is the primary storage of
281 total cell P, with only small amounts stored in phospholipids. P associated with
282 phospholipid partitions to the crude lipid during extraction, while P associated with nucleic
283 acid remains in the primary residual. This explains the large fraction of P found
284 experimentally in the primary residual. The observed increase in P content from dry cells
285 to primary residual (1.39±0.28% to 1.50±0.36%) was not statistically significant, but any
286 increase would demonstrate the disproportional storage of P in non-lipid structures. The
287 92±4% of P found experimentally in the residual correlates with the expected 98% P
288 associated with nucleic acid. We attribute the small amount of P found in the fatty acids to
289 impurities from incomplete partitioning and analytical margin of error.
290
291 *3.2. Oxidation of Organic P to Release Ortho-PO_4^{3-}*

292 Since only small amounts of the starting P were in the crude lipid and subsequent
293 lipid processing, the primary residual became the focus for P recovery. Prior to treatment
294 with H_2O_2 and microwave heating, this primary residual contained 82±1 mg total P with
295 0.2 mg of it as ortho-PO_4^{3-}. After H_2O_2 and microwave treatment, samples contained
296 90±12 mg total P, including 75±6 mg as ortho-PO_4^{3-}. Therefore, H_2O_2 oxidation recovered
297 106±17% of the total P (analytical error accounts for recovery over 100%) and released
298 most of it as ortho-PO_4^{3-}, which was the objective.
299
300 *3.3. Recovery of Ortho-PO_4^{3-} by Resins from DI Water*
301 Figure 3A shows the ability of the two resins to absorb P in DI water. Both resins
302 were able to capture nearly all of the influent P up to 30 bed volumes. At this point, the
303 capacity of the resins was 5.0 mgP/g resin and 4.7 mgP/g resin for the HAX and SBAX
304 resins, respectively. The HAX resin then began a sharp breakthrough and reached
305 complete saturation near 80 bed volumes. The SBAX resin began a gradual breakthrough,
306 reaching 50% saturation around 200 bed volumes and 80% saturation around 500 bed
307 volumes. At the end of the experiments, the HAX resin sorbed a total mass of 38 mg of P,
308 giving a sorption capacity of 11 mgP/g resin, and the SBAX resin sorbed a total mass of
309 140 mg of P, giving a sorption capacity of 40 mgP/g resin.
310 Both resins released all of the P that would be eluted within the first 20 bed
311 volumes of regeneration. They did not release any additional P with 10 additional bed
312 volumes of regeneration (Figure 3B). The fastest rate of P elution for the SBAX resin
313 occurred around 5 bed volumes, and around 8 bed volumes for the HAX resin. A total of
314 19 mg of P was eluted from the HAX resin, or 51% of the total sorbed P was recovered. A

315 total of 167 mg of P was eluted from the SBAX resin, or 119% of the total sorbed was
316 recovered (the lack of mass-balance closure was due to analytical error from high dilution
317 required for analysis of concentrated elute). The pH of the HAX elute containing the
318 recovered P was 12, and of the SBAX elute it was 6.

319 The HAX resin had higher selectivity for P as demonstrated by the lower amount of
320 P in the column effluent, the sharp breakthrough curve showing a short saturation zone,
321 and the higher sorption capacity. We therefore expect it to have a higher rate of P capture
322 in solutions with competing constituents like the oxidized biomass. However, 0.1 N KOH
323 did not efficiently recover the sorbed P. While the iron nanoparticles lead to higher
324 sorption capacity than SBAX, they apparently made it more difficult to desorb the P. Poor
325 recovery might indicate that at least part of the sorbed P was irreversibly adsorbed by the
326 impregnated iron (hydr)oxide nanoparticles instead of sorbed entirely by anion exchange.
327 Our result differs from previous studies that showed that 80-90% of the P could be released
328 by elution from the HAX resin (Martin et al. 2009, Sengupta 2013) using 0.5-1.0 N NaOH
329 plus 0.4 N NaCl. Differences with these previous studies include different influent
330 matrices, not using combined NaCl and NaOH elutes or in as strong doses, and lower resin
331 contact time. We avoided stronger eluent doses so the recaptured P would not be in such a
332 high saline or high pH matrix that it would be unsuitable for subsequent microbial growth.
333 Since elution of the SBAX resin with 0.1 N NaCl showed the best recovery, we focused
334 our subsequent ion-exchange work on it.

335 In order to improve performance with the SBAX resin, we varied column operation
336 parameters to improve the P capture and release. For P capture, a steep breakthrough
337 curve is desired so that all of the P is captured until the inception of breakthrough, at which

time the column is stopped and regenerated. The SBAX breakthrough curve could be made steeper by lowering the hydraulic loading rate. Figure 4 shows results for a SBAX column receiving 100 mgP/L influent in DI water with an EBCT of 20 min (instead of 2 min) and a lower hydraulic loading rate of 3 BV/hr (instead of 30 BV/hr). Consequently, the resin captured all ortho-PO_4^{3-} for 200 BV before exhibiting a steep and desirable breakthrough curve. This gave a sorption capacity of 35.6 mgP/g resin. For P regeneration, slower elution (2 BV/hr) gave 99% recovery of the loaded P within 4 BVs. This allowed us to achieve an 80-fold increase in P concentration in the regenerant. Additional tests (data not shown) indicated greater ortho-PO_4^{3-} exchange capacity at pH 5 instead of 8. This effort aimed to show that each step in this proof-of-concept P-recovery sequence could be optimized to obtain desired performance outcomes.

3.4. Recovery of Ortho-PO_4^{3-} by Resins from Oxidized Biomass

We pumped oxidized primary residual through the ion exchange columns with enough resin so the influent did not exceed 20 bed volumes to ensure complete capture of the P. The HAX column effluent contained 1.7±0.3 mg of P out of the 72±0.9 mgP influent, indicating 98% P capture on the resin. After elution, 16.7±0.0 mg P was in the 100 mL elute. Of this, 14.9±0.1 mg was ortho-PO_4^{3-}. The pH of the pooled elute was 12.4±0.5. Overall, the HAX resin recovered 23%±0.2% of the influent P to the regeneration solution.

The SBAX column effluent contained 20.9±7.6 mg of P out of 108±7.6 mgP influent, indicating 81% of the P sorbed to the resin. After elution, 54.4±8.9 mg of P was in the 100 mL elute. Of this, 53.0±8.2 mg was ortho-PO_4^{3-}. The pH of the pooled elute

361 was 6.6±0.1. Overall, the SBAX resin recovered 50%±5% of the influent P to the
362 regeneration solution.

363 Both resins were only able to recover about half as much P when loaded from
364 oxidized biomass as opposed to when loaded from DI water: HAX went from 51% to
365 23%, and SBAX went from 119% to 50%. Previous studies have also observed lower
366 recovery from complex solutions like sludge liquor than from synthetic solutions (Bottini
367 and Rizzo 2012). In addition to ortho-PO_4^{3-}, the solutions from the oxidized biomass also
368 contained residual organic matter (after oxidation 15 mg P out of 90 mg P was still
369 organic-bound) and other anions (bicarbonate, carbonate, sulfate, and nitrate) that were
370 probably also exchanged by the resins. Additionally, the influent pH for DI tests was 5,
371 but for influent oxidized biomass it was over 6. Having the pH approach the second
372 deprotonation for ortho-PO_4^{3-} ($pK_{a,2}$ = 7.2) during loading shifted a small fraction of its
373 speciation away from the single charge $H_2PO_4^-$ to the double charged HPO_4^{-2}. This may
374 have reduced ortho-PO_4^{3-} adsorption capacity because each HPO_4^{-2} takes up two anion-
375 exchange sites. This effect would be even stronger during regeneration due to the higher
376 pH (12 for the HAX) of the elute when almost all of the ortho-PO_4^{3-} would be present as
377 HPO_4^{-2}. In the case of the HAX resin, this competition for anion exchange sites may have
378 forced more ortho-PO_4^{3-} to be sorbed to the iron (hydr)oxide nanoparticles which could
379 form inner sphere complexes with stronger bonding and less elution.
380
381 *3.5. P Recovery and Reuse*
382 Figure 5 summarizes results for each process step in the overall recovery process
383 using the SBAX resin. The lipid extraction, cellular oxidation, and nutrient isolation steps

384 were, respectively, able to recover 93%, 106%, and 50% (using SBAX) of the starting P.
385 The overall process recovered 54% of the starting intracellular P into a pure and
386 concentrated nutrient solution. This yield is similar to other systems designed for complete
387 P recovery (Blocher et al. 2012) and shows that nutrient reuse in the context of microalgae
388 biofuel production is viable.

389 The recovered solution had an ortho-PO_4^{3-} concentration of 10.6 mgP/L, compared
390 to 5.4 mgP/L required in standard BG-11. We also measured 0.95 mg NO_3^--N/L and 1.5
391 mg SO_4^{2-}-S/L, compared to 247 and 9.8 mg/L required for BG-11, respectively,
392 demonstrating the selectivity of the resin for P.

393 The P solution recovered from the SBAX supported cyanobacteria growth. The
394 optical density increased from 0.12 initially to 0.55 after one day and to 1.11 after one
395 week. This correlates to specific growth rates of 1.4 day^{-1} over one day and 0.7 day^{-1} over
396 one week. For comparison, the optical density of the same cell culture grown in a BG-11
397 solution without any P went from 0.12 initially to 0.16 after one day and 0.10 after one
398 week, corresponding to specific growth rates of 0.26 day^{-1} after one day and -0.06 day^{-1}
399 after one week. The nearly ten-fold increase in cell density over one week in the solution
400 containing recovered P confirms that the recovered P was available for cyanobacteria
401 uptake. It also demonstrates that we did not co-recover any substances that would inhibit
402 reuse, such as harmful heavy metals or residual oxidant. These rates are comparable to
403 growth rates previously observed for *Synechocystis* using BG-11 (Kim et al. 2010) albeit in
404 a different reactor configuration.

405 We recommend future work improving P release methods that can co-recover other
406 valuable products produced by cyanobacteria, like other nutrients, proteins, or ethanol

(Wijffels et al. 2013). We further recommend improving P capture efficiency, reducing the overall cost, energy, and chemical footprint of the process, and demonstrating recovery on full-scale. Other future work could compare the effectiveness of growing microalgae on recovered P compared to other sources of P with complete controls.

4. Conclusions

Efficient P recycling in microbial biofuel production will be essential to preventing competition between food and energy systems. This work demonstrates:

- After lipid processing, over 90% of the P remained in the residuals. Most cellular P is in nucleic acids, with very little in phospholipids.
- Advanced oxidation transformed over 80% of that organic P into useful and recoverable ortho-PO_4^{3-}.
- While HAX resin showed higher affinity for ortho-PO_4^{3-}, the SBAX resin released the ortho-PO_4^{3-} more completely.
- Both resins recovered less P from oxidized biomass than from P spiked DI water, likely due to interference with residual organics or competing oxyanions.

Acknowledgements

A Dean's Fellowship from the Ira A. Fulton Schools of Engineering at Arizona State University provided partial funding for this study, as did the Central Arizona Phoenix Long Term Ecological Research (CAP LTER) project from the National Science Foundation (BCS-1026865). Thank you to Jie Sheng who provided training on lipid

extraction and biofuel processing. Thank you to Chao Zhou and Levi Straka for culturing the cyanobacteria.

References

Batan, L., Quinn, J., Willson, B. and Bradley, T. (2010) Net Energy and Greenhouse Gas Emission Evaluation of Biodiesel Derived from Microalgae. Environmental Science and Technology 44(20), 7975-7980.

Blaney, L.M., Cinar, S. and Sengupta, A.K. (2007) Hybrid Anion Exchanger for Trace Phosphate Removal from Water and Wastewater. Water Research 41(7), 1603-1613.

Blocher, C., Niewersch, C. and Melin, T. (2012) Phosphorus Recovery from Sewage Sludge with a Hybrid Process of Low Pressure Wet Oxidation and Nanofiltration. Water Research 46(6), 2009-2019.

Bottini, A. and Rizzo, L. (2012) Phosphorus Recovery from Urban Wastewater Treatment Plant Sludge Liquor by Ion Exchange. Separation Science & Technology 47(4), 613-620.

Childers, D.L., Corman, J., Edwards, M. and Elser, J.J. (2011) Sustainability Challenges of Phosphorus and Food: Solutions from Closing the Human Phosphorus Cycle. Bioscience 61(2), 117-124.

Clarens, A.F., Resurreccion, E.P., White, M.A. and Colosi, L.M. (2010) Environmental Life Cycle Comparison of Algae to Other Bioenergy Feedstocks. Environmental Science & Technology 44(5), 1813-1819.

Cordell, D., Drangert, J. and White, S. (2009) The Story of Phosphorus: Global Food Security and Food for Thought. Global Environmental Change 19(2), 292-305.

453 de-Bashan, L.E. and Bashan, Y. (2004) Recent advances in removing phosphorus from
454 wastewater and its future use as fertilizer (1997-2003). Water Research 38(19),
455 4222-4246.
456 Elser, J.J., Acharya, K., Kyle, M., Cotner, J., Makino, W., Markow, T., Watts, T., Hobbie,
457 S., Fagan, W., Schade, J., Hood, J. and Sterner, R.W. (2003) Growth Rate
458 Stoichiometry Couplings in Diverse Biota. Ecology Letters 6(10), 936-943.
459 Erisman, J.W., van Grinsven, H., Leip, A., Mosier, A. and Bleeker, A. (2010) Nitrogen and
460 biofuels; an overview of the current state of knowledge. Nutrient Cycling in
461 Agroecosystems 86(2), 211-223.
462 Folch, J., Lees, M. and Stanley, G.H.S. (1957) A Simple Method for the Isolation and
463 Purification of Total Lipids from Animal Tissues. Journal of Biological Chemistry
464 226(1), 497-509.
465 Geider, R. and La Roche, J. (2002) Redfield revisited: Variability of C:N:P in marine
466 microalgae and its biochemical basis. European Journal of Phycology 37(1), 1-17.
467 Hajime, W. and Murata, N. (2007) The Essential Role of Phosphatidylglycerol in
468 Photosynthesis. Photosynthesis Research 92(2), 205-215.
469 Huo, Y.-X., Wernick, D.G. and Liao, J.C. (2012) Toward nitrogen neutral biofuel
470 production. Current Opinion in Biotechnology 23(3), 406-413.
471 Kaneko, T., Sato, S., Kotani, H., Tanaka, A., Asamizu, E., Nakamura, Y., Miyajima, N.,
472 Hirosawa, M., Sugiura, M., Sasamoto, S., Kimura, T., Hosouchi, T., Matsuno, A.,
473 Muraki, A., Nakazaki, N., Naruo, K., Okumura, S., Shimpo, S., Takeuchi, C.,
474 Wada, T., Watanabe, A., Yamada, M., Yasuda, M. and Tabata, S. (1996) Sequence
475 Analysis of the Genome of the Unicellular Cyanobacterium Synechocystis sp.

476 Strain PCC6803. II. Sequence Determination of the Entire Genome and
477 Assignment of Potential Protein-coding Regions. DNA Research 3(3), 109-136.
478 Kim, W.K., Vannela, R., Zhou, C., Harto, C. and Rittmann, B.E. (2010) Photoautotrophic
479 Nutrient Utilization and Limitation During Semi-Continuous Growth of
480 Synechocystis sp. PCC6803. Biotechnology and Bioengineering 106(4), 553-563.
481 Liao, P.H., Wong, W.T. and Lo, K.V. (2005) Advanced Oxidation Process Using
482 Hydrogen Peroxide/Microwave System for Solubilization of Phosphate. Journal of
483 Environmental Science and Health 40(9), 1753-1761.
484 Martin, B.D., Parsons, S.A. and Jefferson, B. (2009) Removal and Recovery of Phosphate
485 from Municipal Wastewater Using a Polymeric Anion Exchanger Bound with
486 Hydrated Ferric Oxide Nanoparticles. Water Science and Technology 60(10),
487 2637-2645.
488 Mata, T.M., Martins, A.A. and Caetano, N.S. (2010) Microalgae for Biodiesel Production
489 and Other Applications: A Review. Renewable & Sustainable Energy Reviews
490 14(1), 217-232.
491 Midorikawa, I., Aoki, H., Omori, A., Shimizu, T., Kawaguchi, Y., Kassai, K. and
492 Murakami, T. (2008) Recovery of High Purity Phosphorus from Municipal
493 Wastewater Secondary Effluent by a High Speed Adsorbent. Water Science and
494 Technology 58(8), 1601-1607.
495 Miner, G. (2006) Standard Methods for the Examination of Water and Wastewater, 21st
496 Edition, American Water Works Association.
497 Morse, G.K., Brett, S.W., Guy, J.A. and Lester, J.N. (1998) Review: Phosphorus Removal
498 and Recovery Technologies. The Science of the Total Environment 212(1), 69-81.

499 Rees-Nowak, D., Marston, C. and Gisch, D. (2005) Controlling Chromium. Water &
500 Wastewater International 20(5), 21.
501 Rippka, R., Deruelles, J., Waterbury, J.B., Herdman, M. and Stanier, R.Y. (1979) Generic
502 Assignments, Strain Histories And Properties Of Pure Cultures Of Cyanobacteria.
503 Journal of General Microbiology 111(Mar), 1-61.
504 Rittmann, B.E. (2008) Opportunities for renewable bioenergy using microorganisms.
505 Biotechnology and Bioengineering 100(2), 203-212.
506 Rittmann, B.E., Mayer, B., Westerhoff, P. and Edwards, M. (2011) Capturing the lost
507 phosphorus. Chemosphere 84(6), 846-853.
508 Sakurai, I., Shen, J., Leng, J., Ohashi, S., Kobayashi, M. and Wada, H. (2006) Lipids in
509 Oxygen Evolving Photsystems II Complexes of Cyanobacteria and Higher Plants.
510 Journal of Biochemistry 140(2), 201-209.
511 Schenk, P.M., Thomas-Hall, S.R., Stevens, E., Marx, U.C., Mussgnug, J.H., Posten, C.,
512 Kruse, O. and Hankamer, B. (2008) Second Generation Biofuels: High Efficiency
513 Microalgae for Biodiesel Production. Bioenergy Research 1(1), 20-43.
514 Sengupta, S. (2013) Novel Solutions to Water Pollution. Ahuja, S. and Hristovski, K.
515 (eds), pp. 167-187, American Chemical Society, Washington DC.
516 Shastri, A.A. and Morgan, J.A. (2005) Flux Balance Analysis of Photoautotrophic
517 Metabolism. Biotechnology 21(6), 1617-1626.
518 Sheng, J., Kim, H.W., Badalamenti, J.P., Zhou, C., Sridharakrishnan, S., Krajmalnik-
519 Brown, R., Rittmann, B.E. and Vannela, R. (2011a) Effects of Temperature Shifts
520 on Growth Rate and Lipid Characteristics of Synechocystis sp. PCC6803 in a
521 Bench-Top Photobioreactor. Bioresource Technology 102(24), 11218-11225.

522 Sheng, J., Vannela, R. and Rittmann, B.E. (2011b) Evaluation of Methods to Extract and
523 Quantify Lipids from Synechocystis PCC6803. Bioresource Technology 102(2),
524 1697-1703.
525 Soh, L. and Zimmerman, J. (2011) Biodiesel Production: The Potential of Algal Lipids
526 Extracted with Supercritical Carbon Dioxide. Green Chemistry 13(6), 1422-1429.
527 Sterner, R.W. and Elser, J.J. (2002) Ecological Stoichiometry: The Biology of Elements
528 from Molecules to the Biosphere, Princeton University Press, Princeton, New
529 Jersey.
530 Stucker, V., Ranville, J., Newman, M., Peacock, A., Cho, J. and Hatfield, K. (2011)
531 Evaluation and application of anion exchange resins to measure groundwater
532 uranium flux at a former uranium mill site. Water Research 45(16), 4866-4876.
533
534 Takahashi, H., Uchimiya, H. and Hihara, Y. (2008) Difference in metabolite levels
535 between photoautotrophic and photomixotrophic cultures of Synechocystis sp. PCC
536 6803 examined by capillary electrophoresis electrospray ionization mass
537 spectrometry. Journal of Experimental Botany 59(11), 3009-3018.
538 United States Environmental Protection Agency (USEPA) (2008) Test Methods for
539 Evaluating Solid Waste, Physical/Chemical Methods, Washington D.C.
540 United States Geological Survey (USGS) (2011) Mineral Commodity Summaries 2011,
541 Reston, VA.
542 van de Meene, A.M.L., Hohmann-Marriott, M.F., Vermaas, W.F.J. and Roberson, R.W.
543 (2006) The three-dimensional structure of the cyanobacterium Synechocystis sp
544 PCC 6803. Archives of Microbiology 184(5), 259-270.

545 Vermaas, W. (1996) Molecular Genetics of the Cyanobacterium Synechocystis sp. PCC
546 6803: Principles and Possible Biotechnology Applications. Journal of Applied
547 Phycology 8(4-5), 263-273.
548 Vermaas, W.F.J. (2001) Encyclopedia of Life Sciences, pp. 245-251, John Wiley & Sons,
549 Ltd, London.
550 Wijffels, R.H., Kruse, O. and Hellingwerf, K.J. (2013) Potential of Industrial
551 Biotechnology with Cyanobacteria and Eukaryotic Microalgae. Current Opinion in
552 Biotechnology 24(3), 405-413.
553 Wong, W.T., Chan, W.I., Liao, P.H., Lo, K.V. and Mavinic, D.C. (2006) Exploring the
554 Role of Hydrogen Peroxide in the Microwave Advanced Oxidation Process;
555 Solubilization of Ammonia and Phosphates. Journal of Environmental Engineering
556 and Science 5(6), 459-465.

557

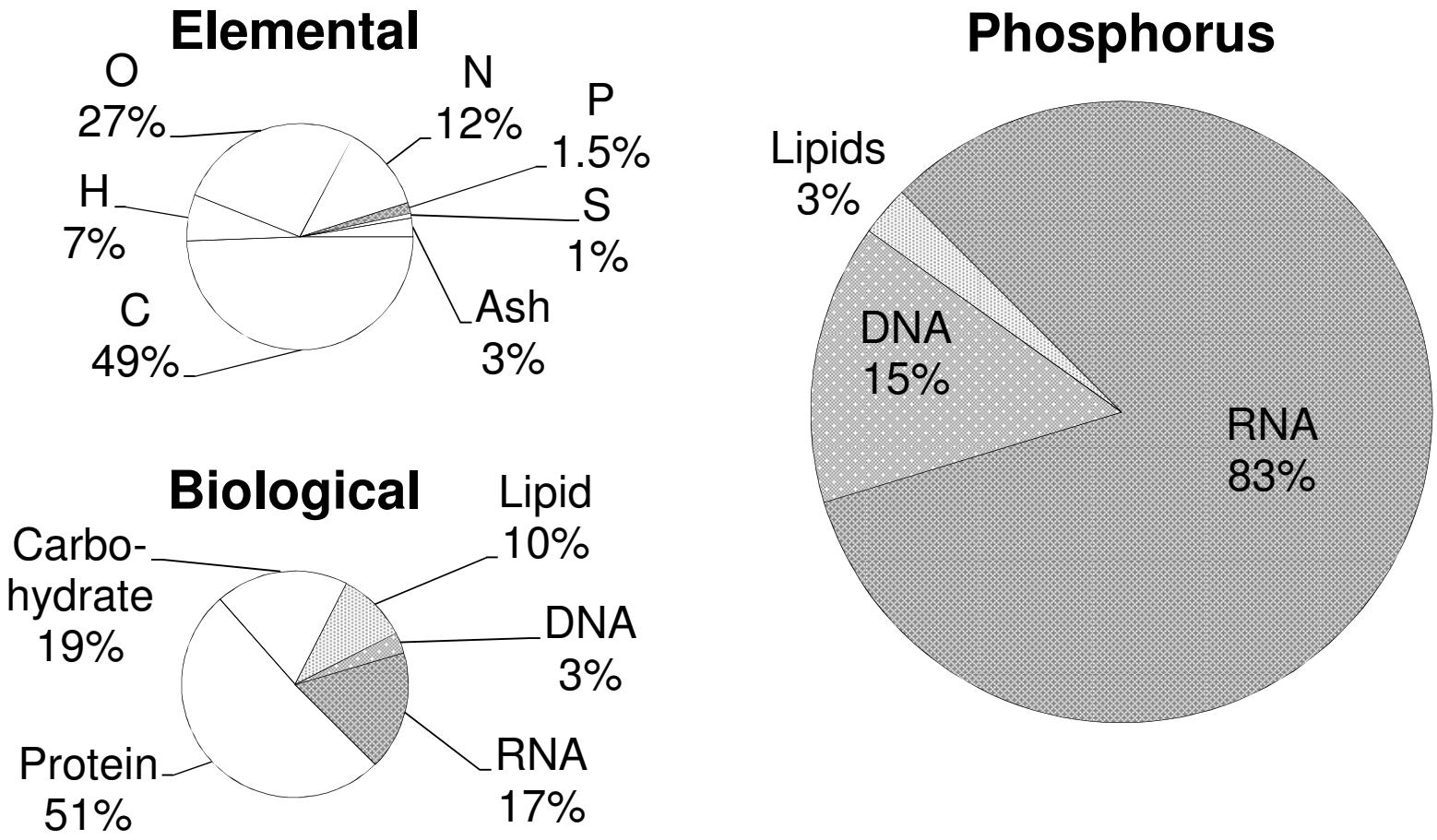

Figure 1 – The estimated location of P within *Synechocystis* sp. PCC 6803 shown on the right determined by the elemental (Kim et al. 2010) and biological (Shastri and Morgan 2005) composition shown on the left. All numbers given are percent by weight of the total biomass (left) or total P in the biomass (right). A majority of cellular P is in RNA, and only small amounts are in lipids. Thus, almost all P is in the primary residuals after lipid extraction, not in the lipid extract.

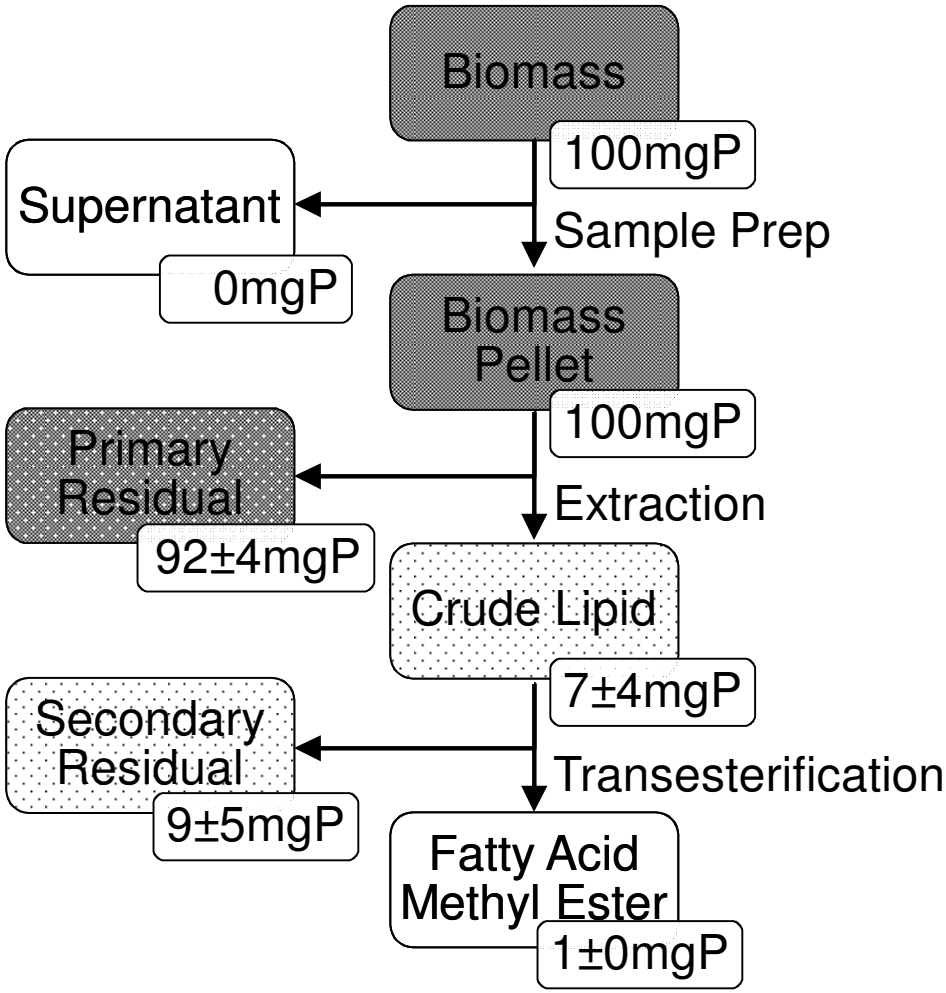

Figure 2 – The fate of 100 mg of starting P through the lipid extraction process. Most of the P remained with the biomass in the primary residual, although some was associated with the crude lipid remains in the secondary residual. The FAME only contained about 1% of the starting P.

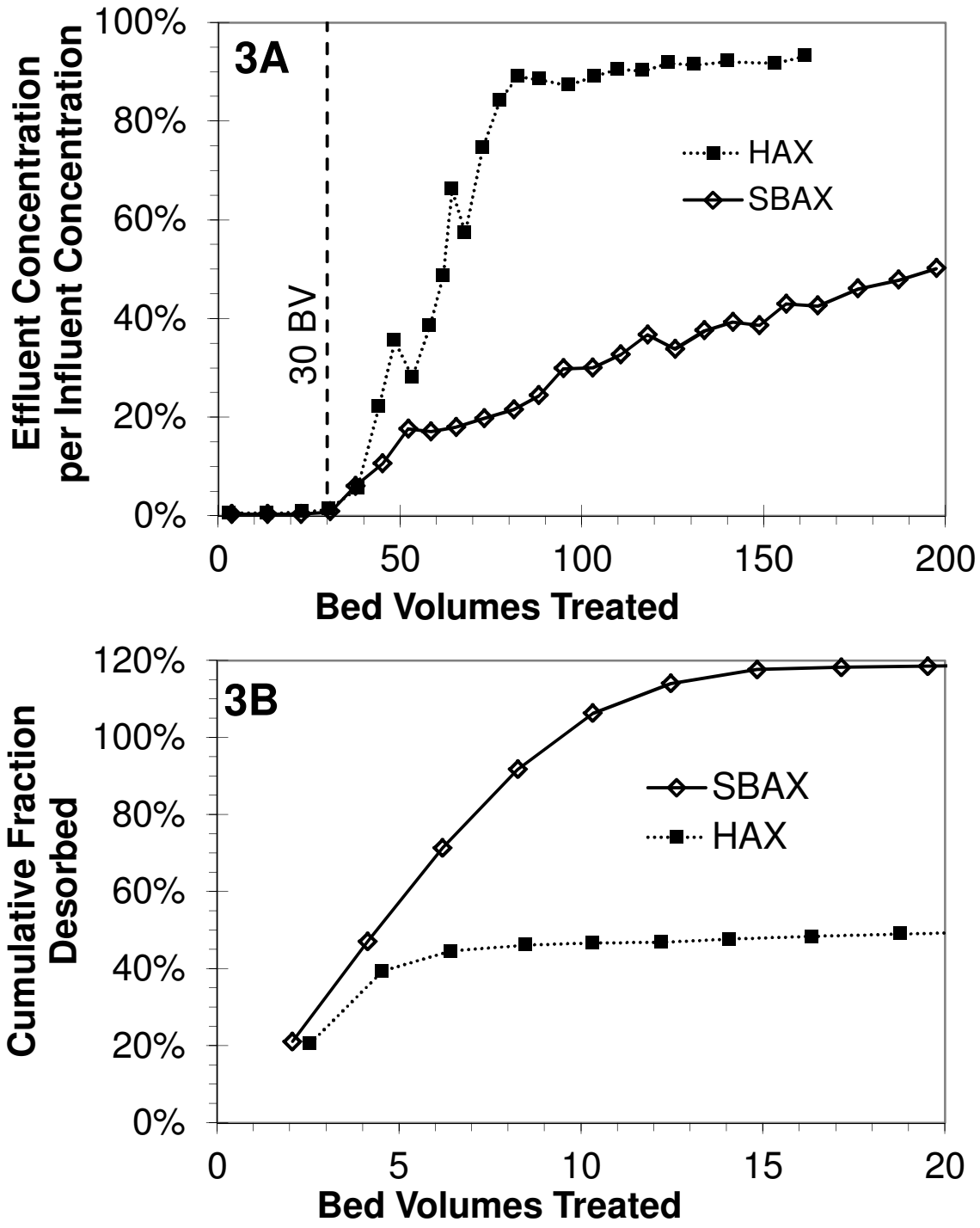

Figure 3 – Performance of an iron hydr(oxide) impregnated anion exchange (HAX) resin (squares) and a strong-base anion exchange (SBAX) resin (diamonds) for recovering phosphate from DI water. (A) Uptake of phosphate by fresh resin in column test. Uses hydraulic loading rate of 30 BV/hr, an initial P concentration of 80 mgP/L, and influent pH 5. (B) Desorption of phosphate from resin by 0.1 N KOH for HAX or 0.1 N NaCl for SBAX with hydraulic loading rate of 6 BV/hr, normalized to mass of P sorbed. The HAX resin shows higher affinity for P during sorption, but the SBAX releases more P upon elution.

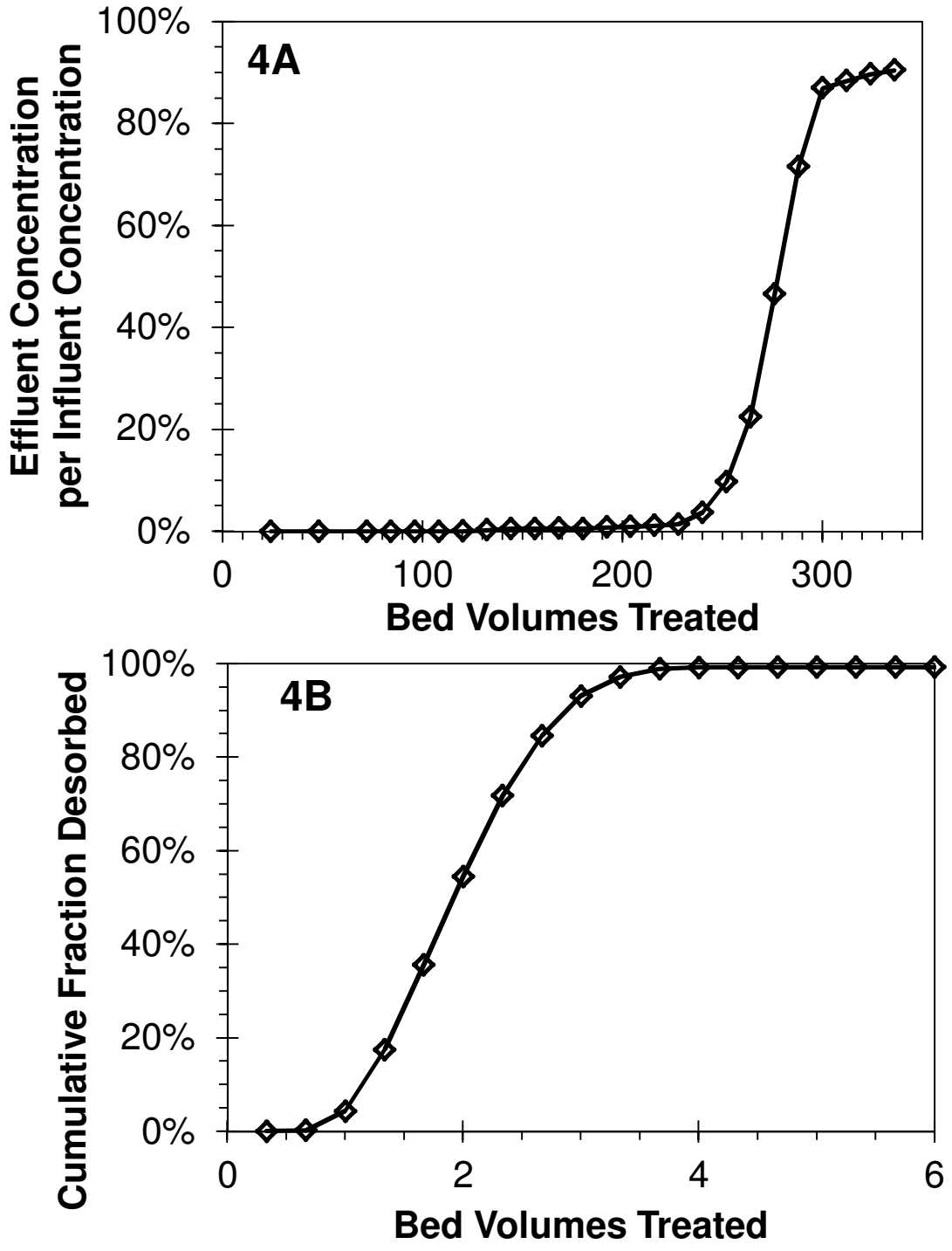

Figure 4 – Enhanced P recovery from DI water on SBAX resin by improving operating conditions. (A) Uptake of phosphate by fresh resin in column test. Uses hydraulic loading rate of 3 BV/hr, an initial P concentration of 100 mgP/L, and influent pH 8. (B) Desorption of phosphate from resin by 1 N NaCl at a hydraulic loading rate of 2 BV/hr, normalized to mass P sorbed. The steep breakthrough after a long bed run is optimal for P recovery, and subsequent elution in few bed volumes gives an 80-fold increase in P concentration.

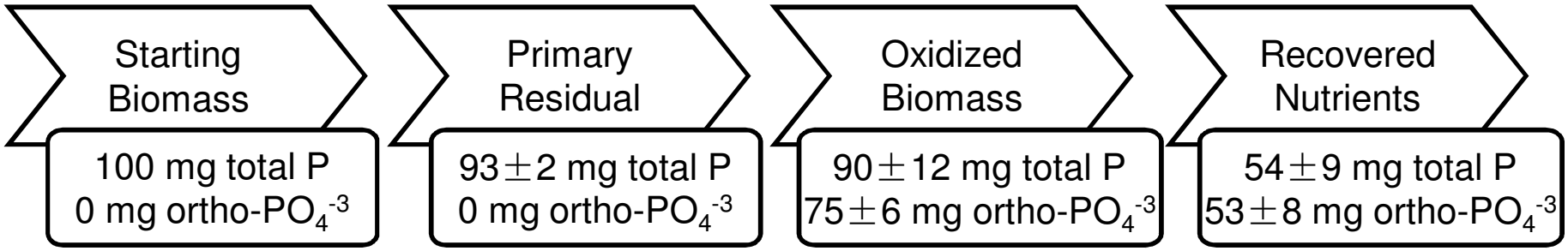

Figure 5 – Process step yields of total P and ortho-PO_4^{3-} for 100 mg starting P through the P-recovery process using advanced oxidation and SBAX. Nearly all cellular P was found in the primary residual after lipid extraction. Advanced oxidation transformed a majority of the P to recoverable and beneficial ortho-PO_4^{3-}. SBAX resin could then sorb and elute a concentrated nutrient solution. The overall tested P-recovery process could capture more than 50% of the starting P in a beneficial form.

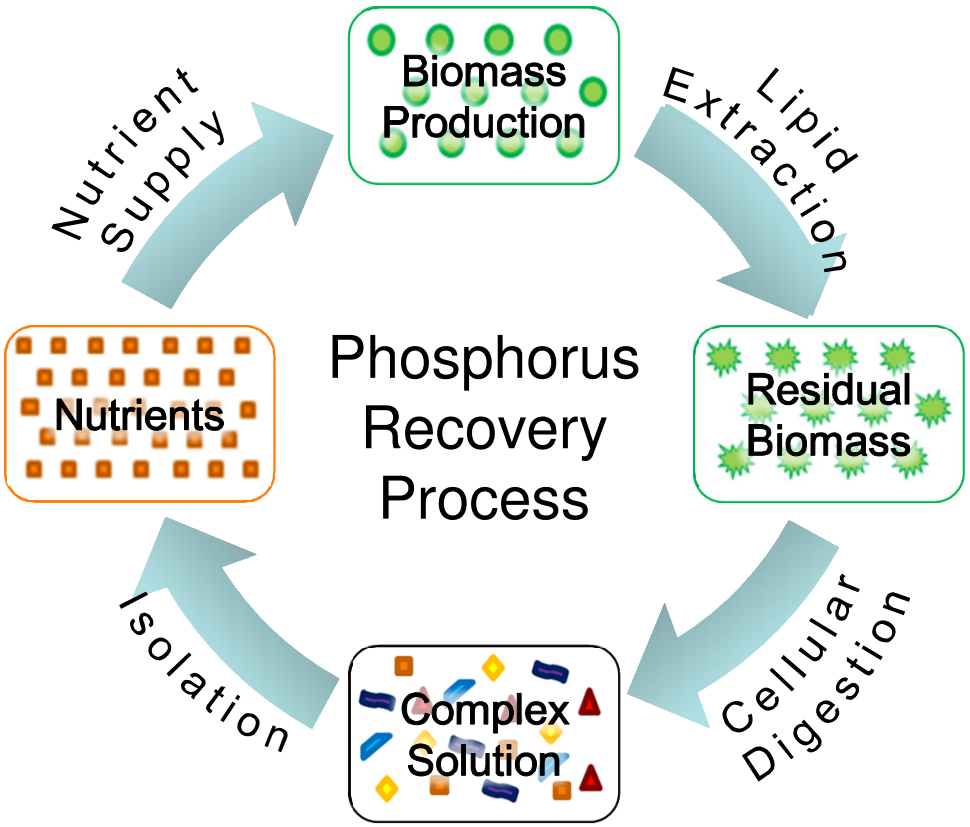
Biomass Production
Lipid Extraction
Residual Biomass
Cellular Digestion
Complex Solution
Isolation
Nutrients
Nutrient Supply
Phosphorus Recovery Process